Hollow Fiber Compression Technique: A Historical Perspective

Mauro Nisoli

(Invited Paper)

***Abstract*—This review analyzes the evolution, applications, and future prospects of the hollow fiber compression technique, a pivotal advancement in ultrafast laser technology. Over the past three decades, this technique has emerged as a cornerstone, proving instrumental in the generation of few-cycle pulses characterized by millijoule-level energy, spanning a wide spectral range from ultraviolet to mid-infrared wavelengths. Its versatility and efficiency have found applications in diverse scientific disciplines, ranging from attosecond science to extreme nonlinear optics. The review delves into the historical development of the hollow fiber compression technique, highlighting key milestones and technological breakthroughs that have contributed to its current status. The widespread adoption of this technique in laboratories on a global scale is investigated, and an exploration is conducted into the continuously reported innovative experimental implementations. The impact of this technique on attosecond science is scrutinized, emphasizing its role in the generation and application of isolated attosecond pulses.**

***Index Terms*—Hollow fiber compression, few-cycle pulses, ultraviolet to mid-infrared wavelengths, attosecond science, extreme nonlinear optics.**

I. Introduction

HIGH-ENERGY few-optical-cycle pulses are of crucial importance for a large variety of high-field applications: from the investigation of extreme nonlinear processes in matter to the generation of ultrashort pulses in the extreme-ultraviolet (EUV) spectral region. As discussed by Fattahi et al. [1], the second-generation femtosecond technology, based on chirped-pulse amplification (CPA) typically in Ti:sapphire-based laser systems, has catalyzed the emergence of novel research domains. Noteworthy among these are attosecond science and technology [2], [3], [4], as well as laser-driven particle acceleration [5]. The third-generation femtosecond technology, which will be characterized by high (terawatt-scale) peak powers with high (kilowatt-scale) average powers in ultrashort optical pulses, promises to pave the way to completely unexplored research fields. Optical parametric CPA (OPCPA) [6], in particular, stands out as a pivotal technology capable of generating high-energy pulses with durations in the few-cycle regime, serving as the foundational framework for the third-generation femtosecond technology.

A distinct and complementary avenue for generating high-energy few-cycle pulses involves the implementation of post-compression techniques. After nearly three decades since its invention, the hollow-capillary fiber (HCF) compression technique [7] continues to be the primary method for compressing high-energy pulses, achieving sub-5-fs durations. Despite the introduction of various alternative and promising techniques in recent years [8], such as the utilization of multi-pass cells [9], the HCF compression technique continues to be the most widely employed approach. This compression scheme achieves spectral broadening by injecting a laser pulse into a gas-filled glass capillary, characterized by an inner diameter ranging from a few tens of micrometers to a few millimeters. Dispersion compensation is then obtained by employing broadband compressors, typically made by chirped mirrors. Pulses with energies of the orders of a few millijoules (even tens of millijoules), in different spectral regions, from ultraviolet (UV) to mid-infrared (mid-IR), have been compressed by using the HCF technique. Another noteworthy feature of this experimental approach, especially crucial for various applications in attosecond technology, is that the propagation along a gas-filled capillary does not compromise the stability of the carrier-envelope phase (CEP) of the pulses, provided that the experimental setup is appropriately designed.

The fundamental concept of pulse compression follows a straightforward procedure: initially, the input pulse is introduced into a phase modulator, which broadens the pulse spectrum by inducing a time-dependent frequency sweep. Such phase modulator must be extremely fast, ideally instantaneous, to effectively modulate the phase of ultrashort pulses. Subsequently, the newly generated frequency components resulting from the phase modulation are re-phased through the implementation of a broadband dispersive delay line. This compression scheme was independently proposed by Gires and Tournois in 1964 [10] and Giordmaine et al. in 1968 [11]. Self-phase modulation (SPM) is generally used to modulate the temporal phase of a pulse, as proposed in the case of picosecond pulses in 1969 by Fisher et al. [12]. A key requisite is a uniform SPM, and therefore a uniform spectral broadening, across the transverse spatial profile of the laser beam. Spatially uniform SPM can be achieved

Manuscript received 6 February 2024; revised 28 February 2024; accepted 29 February 2024. Date of publication 5 March 2024; date of current version 15 March 2024. This work was supported by the European Research Council under ERC Grant 951224 TOMATTO.

The author is with the Department of Physics, Politecnico di Milano, 20133 Milano, Italy, and also with the Institute of Photonics and Nanotechnologies, National Research Council, 20133 Milano, Italy (e-mail: mauro.nisoli@polimi.it).

Color versions of one or more figures in this article are available at https://doi.org/10.1109/JSTQE.2024.3373174.

Digital Object Identifier 10.1109/JSTQE.2024.3373174

by employing a guiding nonlinear medium. In 1974 Ippen et al. reported on the first measurement of SPM in a guiding multimode optical fiber filled with liquid CS_2 [13]. In 1978 Stolen and Lin reported measurements of SPM in single-mode fibers [14]. In 1981 Nakatsuka et al. [15] demonstrated the first pulse compression experiment using fibers as a Kerr medium.

In order to avoid damage, fused silica fibers can be used to spectrally broaden pulses with a maximum energy of a few tens of nanojoules. The HCF compression technique was introduced to overcome this problem: guiding propagation is obtained by grazing incidence reflection at the dielectric inner surface of the capillary and spectral broadening is achieved in noble gases, characterized by a high damage threshold (related to its ionization) and an instantaneous nonlinearity (related to purely electronic processes). This work is devoted to an historical overview of the hollow fiber compression technique. Various experimental implementations and applications will be discussed, which have been proposed and demonstrated in the last two decades.

This review is structured as follows: In Section II, we explore the origins of the foundational concepts underlying the invention of the HCF technique and its initial experimental implementations. Section III provides an analysis of the energy scalability of this compression method up to the Terawatt (TW) scale. In Section IV, we introduce two distinct schemes for generating supercontinua in HCFs: the HCF cascading and the light field synthesizer. Section V focuses on the compression of high-energy pulses in the IR spectral region. Additionally, Section VI details the generation of ultrashort pulses with wide tunability in the UV and Deep UV (DUV) spectral regions by implementing resonant dispersive wave (RDW) emission in gas-filled HCFs. Section VII delves into the use of molecular gases for spectral broadening and pulse compression. Finally, Section VIII reviews the initial applications of compressed pulses in strong-field phenomena, namely high-order harmonic generation and strong-field ionization.

II. HCF Compression Technique: Conceptual Genesis and Initial Demonstrations

A. *Origins of the HCF Compression Technique: Unveiling Its Inception*

Rolland and Corkum [16] were the first to explore the compression of laser pulses with energies in the microjoule range. The concept of their approach involved substituting the single-mode optical fiber, which was conventionally utilized for spectral broadening, with a compact nonlinear bulk material, specifically quartz. To mitigate the adverse impact of self-focusing, they employed short lengths of quartz and large incident-beam sizes. In addition to the energy scalability constraints imposed by the damage threshold of the bulk medium, this methodology faced a significant limitation concerning the non-uniform spectral broadening observed across the transverse spatial profile of the laser beam. To address this challenge, a small aperture was placed immediately after the quartz to select a region of the output beam characterized by a nearly constant intensity profile. As the aperture size was enlarged, there was a noticeable decrease in the measured spectral width along with a deterioration in the temporal intensity profile of the pulse. This occurred because the small spectral broadening generated in the low-intensity regions of the transverse spatial intensity profile of the beam began to contribute to the radiation transmitted through the aperture. Consequently, a trade-off between spectral broadening and output pulse energy becomes necessary to optimize the system. Utilizing this technique, compressed pulses with energies in the tens of microjoules range and durations of less than 24 fs, corresponding to a compression factor of approximately four with an energy efficiency of around 10%, were achieved.

An inspiring work was published in 1995 by Braun and colleagues [17]. Self-channeling of high-peak-power femtosecond laser pulses through 20 m of air was demonstrated. The energy, diameter and broadened spectrum of the self-channeled ultrashort pulses were measured to be fairly constant during the propagation. Filamentation arises from an intricate dynamical interplay primarily involving the Kerr effect (comprising self-focusing, SPM and self-steepening), photoionization (involving absorption and defocusing), and linear effects (including diffraction and dispersion). During filamentation, SPM widens the spectrum of the incident pulse to over an optical octave, while self-guiding functions as a spatial filter, resulting in enhanced spatial mode quality. It is worth mentioning that the use of gases for spectral broadening of ultrashort pulses was first reported in 1986 by Corkum and colleagues [18]. They demonstrated the generation of supercontinua spanning from UV to IR wavelengths. This was achieved by focusing 2-ps or 70-fs pulses with an energy $\leq 500\ \mu$J into a high-pressure cell filled with noble gases (specifically Ar, Kr, and Xe) as well as molecular gases (H_2, N_2, and CO_2), with pressures ranging from 1 to 40 atm.

The observation of femtosecond pulse filamentation over extended distances in gases marked a significant advancement. It sparked the idea of guiding high-energy pulses through a nonlinear medium with a higher "damage threshold" compared to solid media. A critical challenge remained to be addressed: how to maintain, in the case of gases, the key characteristic of single-mode optical fibers, namely, the presence of a propagation mode characterized by uniform spectral broadening across the entire beam cross-section?

The latest and fundamental idea was to replace single-mode optical fiber with what had been introduced in the 1960 s for optical transmission over long distances before the introduction of optical fibers: the hollow metallic and dielectric waveguides. The field configuration and propagation constants of the normal modes in hollow circular waveguides with diameters much larger than wavelength were studied by Marcatili and Schmeltzer [19]. We immediately opted for dielectric HCFs, since in this case the lowest loss mode is the hybrid mode EH_{11}, which is a quasi-linearly polarized mode (departures from linear polarization can be observed for very small capillaries), while for metallic HCFs the mode with the lowest attenuation is the transverse circular electric mode TE_{01} in which the electric field lines are transverse concentric circles centered on the propagation axis. For this reason we tested various fused silica HCFs manufactured at the Optoelectronics Research Center of the University of Southampton.

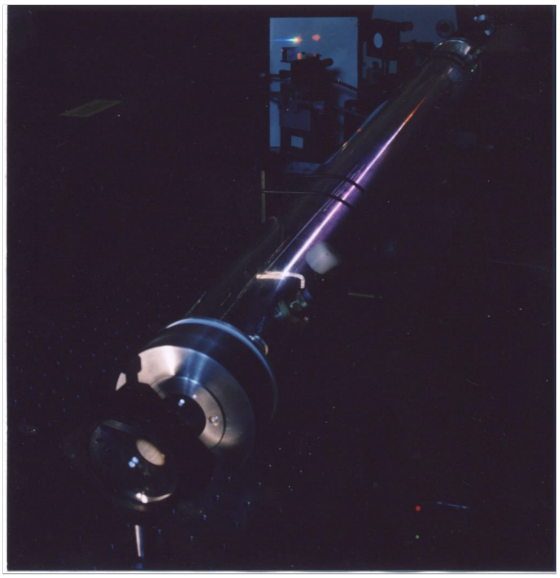

Fig. 1. Photograph of the first implementation of the hollow fiber compressor at the Department of Physics of Politecnico di Milano. The fiber was kept straight in a V-groove made in an aluminum bar, which was then placed in a plexiglass tube with quartz windows, filled with noble gases.

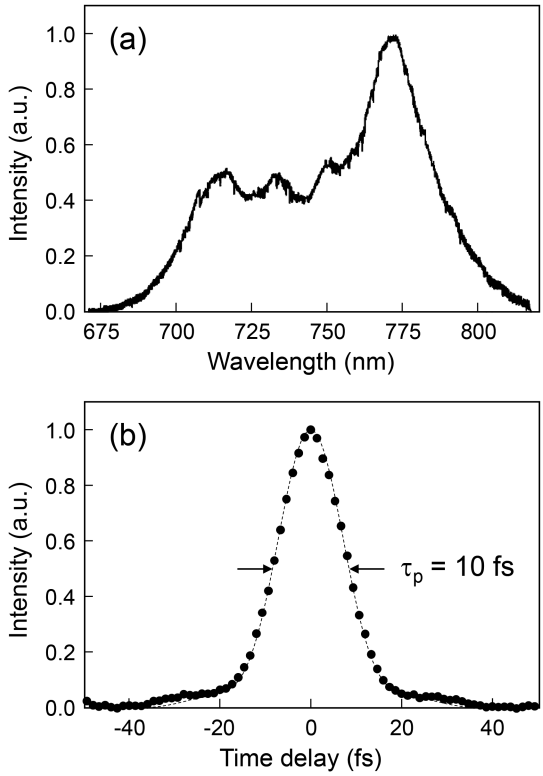

Fig. 2. First experimental demonstration of the hollow fiber compression technique. (a) Portion of the spectrum at the output of the fiber filled with krypton at a pressure $p = 2$ atm and at a pulse peak intensity $P_0 = 3.5$ GW. (b) Temporal characterization of the compressed pulse by second-harmonic intensity autocorrelation. The dots correspond to the experimental data, the dashed curve represents the autocorrelation trace of the transform-limited pulses. Pulse duration was estimated assuming a sech^2 pulse shape.

B. First Experimental Demonstrations of the HCF Compression Technique

Fig. 1 displays the photograph depicting the initial implementation of the hollow fiber compressor at the Department of Physics of Politecnico di Milano. 140-fs laser pulses at a central wavelenght of 780 nm, with an energy of 0.66 mJ were injected into a 70-cm-long capillary with an inner diameter of 140 μm, filled with noble gases [7]. The coupling efficiency measured at the output of the high pressure chamber, was about 50%. Dispersion compensation was achieved by double pass through a Brewster angle quartz prism pair. A first set of experiments was performed by using argon at a pressure $p = 7$ bar. Substantial spectral broadening was achieved, featuring pronounced amplitude modulations characteristic of the SPM process. Pulses as short as 13 fs were attained, exhibiting minimal side lobes and low-intensity tails. Due to the higher Kerr nonlinearity of xenon compared to argon, similar results were also found with xenon at lower pressure ($p = 3$ bar). The use of the latter gas was however limited by the onset of multiphoton ionization.

The most favorable outcomes in terms of spectral broadening were obtained by employing krypton at a pressure $p = 2$ bar, resulting in an overall spectral broadening of up to approximately 200 nm. We immediately encountered the primary limitation of the experimental setup, which was related to compensating for dispersion across an ultrabroad spectral bandwidth. The challenge arose from employing dispersion compensation based on prism pairs. While this method effectively introduced negative group delay dispersion (GDD), it also led to a significant amount of higher-order dispersion. Unfortunately, adjusting or reducing this higher-order dispersion independently of the desired GDD was not feasible, thereby limiting the bandwidth over which accurate dispersion control could be achieved. Furthermore, utilizing prisms at high power levels was problematic due to the onset of unwanted nonlinearities within the prism material. Best results in terms of pulse duration and time-bandwidth product were achieved by selecting the central portion of the output spectrum, as depicted in Fig. 2(a), by using a slit with adjustable width positioned in the symmetry plane of the prism sequence employed for dispersion compensation. Based on the intensity autocorrelation function depicted in Fig. 2(b) and assuming a sech^2 pulse shape, a pulse duration of 10 fs was measured, which corresponds to the transform limited value. Pulse amplitude fluctuations were below 5% and beam divergence, due to spatial filtering of the hollow fiber, was very close to diffraction limit.

A second set of experiments was performed by employing 20-fs input pulses with an energy of 40 μJ. A 60-cm-long fiber was used, with an inner diameter of 160 μm, filled with krypton [20]. Dispersion compensation was obtained by using a dispersive delay line formed by chirped mirrors and two pairs of fused silica prisms of small apex angle (20°). The compressed pulses were measured by interferometric second harmonic autocorrelation: pulses as short as 4.5 fs were measured. Scaling the input energy to higher values, the generation of sub-10-fs pulses at the sub-terawatt peak power level was then demonstrated [21]. 20-fs input pulses with an energy of 1 mJ were coupled into a 60-cm-long, 500-μm diameter hollow

fiber, filled with argon. Dispersion compensation was achieved by using chirped mirrors. Pulses as short as 5 fs were obtained with an energy of 0.55 mJ, thus corresponding to a peak power of 0.11 TW.

III. Energy Scalability

In the design of an HCF compressor, two key constraints must be considered [22]. Firstly, the maximum pulse peak power, P_0, is bounded by the critical power for self-focusing, P_{cr}. This limitation ensures a weak coupling from the fundamental transverse mode of the fiber to higher-order modes. The critical power is expressed as $P_{cr} = \lambda^2/(2\kappa_2 p)$, where λ is the wavelength, and κ_2 is the ratio between the nonlinear index coefficient and the gas pressure p [23]. Additionally, ionization effects must be accounted for. To ensure the proper operation of the HCF compression, it is important that the change in refractive index induced by the Kerr effect ($\Delta n = \kappa_2 p I$) significantly surpasses the refractive index change induced by gas ionization. These constraints collectively give rise to a straightforward scaling law [8]

$$P_0 \propto \frac{1}{\kappa_2 p} \propto a^2 \propto L \tag{1}$$

where a and L are the inner radius and the length of the fiber, respectively. Based on this simple and rather conservative scaling law, various experimental methodologies have been introduced over the years to enable the use of this compression technique with high-energy pulses, including those reaching into the tens of millijoules. In the following we will discuss the main methodologies that have now become standard in various research laboratories. In particular, in Section III-A we will analyze the use of pressure gradients within the fiber, which was introduced to mitigate the negative effects of excessive gas ionization at the input of the fiber. In Section III-B we will discuss the use of capillaries with lengths of several meters, made possible by the introduction of stretched fibers, which enables to arbitrarily increase the HCF length without compromising its waveguiding properties. Finally, in Section III-C we will mention the use of circularly polarized pulses.

Here it is worth mentioning a different approach, although less commonly employed, to enhance the energy scalability of the HCF compression technique based on the implementation of pulse division. In this method, the input pulse is initially temporally divided into a series of nearly identical sub-pulses, which are then individually coupled into gas-filled HCFs for independent spectrum broadening. Finally, the sub-pulses are recombined into a single pulse and compressed temporally. Wang and colleagues conducted theoretical investigations into this method, illustrating its suitability for compressing ultrafast pulses with energies significantly exceeding the millijoule level down to a few cycles [24]. Previously this idea was applied to nonlinear pulse compression by using SPM into a piece of undoped rod-type fiber [25] and in a solid-core fiber [26]. The extension of this technique to gas-filled HCFs was reported by Jacqmin et al. with the first experimental demonstration of optical multiplexing of few-cycle pulses in a HCF compressor [27]. Passive coherent combining of two temporally divided pulse replicas, each with an energy of 500 μJ and a duration of 29 fs, was successfully demonstrated. These pulses underwent spectral broadening within a neon-filled hollow fiber compressor, achieving an impressive combining efficiency of 95%. After dispersion compensation using a pair of thin fused-silica wedges and a set of chirped mirrors, pulses as short as 6 fs were measured.

A. HCF Compression Using Pressure Gradients

To avoid the generation of large electron density gradients, with detrimental consequences on the performances of the HCF setup, in 2005 Suda and co-workers introduced the so-called pressure gradient configuration, where the gas pressure increases along the capillary [28]. The input pressure is kept to a minimum value by continuous pumping. The main advantages of this configuration are the following: (i) free electron density at the fiber input (where pulse intensity is maximum) is strongly reduced, thus increasing the coupling efficiency of the fundamental mode; (ii) self-focusing can be significantly prevented or delayed, while enhancing the energy transmittance [29], [30]. A 220-cm-long HCF with an inner radius of 250 μm was used, filled with argon. The pressure at the input of the fiber was kept to a few mbars and to 40 kPa at the output. 40-fs pulses, with an energy of 8.5 mJ generated by a Ti:sapphire amplified laser system working at 10-Hz repetition rate were focused at the entrance of the fiber. Dispersion compensation was achieved by using chirped mirrors. Pulse duration of the compressed pulses was measured by using a single-shot autocorrelator: pulses as short as 9.8 fs were obtained with an energy of 5 mJ, with a pedestal due to uncompensated higher-order dispersion.

In order to achieve a further reduction of the ionization of the gaseous medium, chirped pulses were used for spectral broadening in a HCF with pressure gradient [31]. By using helium as a nonlinear medium, pulses as short as 5 fs were generated with an energy of 5 mJ (at 1-kHz repetition rate). The maximum peak intensity at the fiber input, which must be kept below the ionization threshold, was first estimated by measuring the broadened spectra at a given pressure, upon increasing the input pulse energy. Above the ionization threshold a clear ionization-induced blue shift in the spectrum was produced: the spectral broadening was almost clamped and the spectral profile became asymmetric. The maximum peak intensity, I_{th}, was estimated of the order of 2×10^{14} W/cm^2 for neon and 4×10^{14} W/cm^2 for helium. Upon introducing a chirp on the input pulses it is possible to significantly increase the maximum pulse energy, $\mathcal{E}_{\max}$, keeping the peak intensity below I_{th}. An estimation of the maximum energy, in excellent agreement with experimental results, is given by the following simple expression [31]:

$$\mathcal{E}_{\max} = \pi a^2 I_{th} \tau_0 \sqrt{1 + \left(4 \ln 2 \frac{\phi''}{\tau_0^2}\right)^2} \tag{2}$$

where: πa^2 is the effective beam area inside the fiber; τ_0 is the Fourier-transform limited pulse duration (FWHM); ϕ'' is the GDD.

B. Spectral Broadening in Stretched Flexible HCFs

In order to preserve a large spectral broadening without increasing the ionization rate, it is useful to increase the length of the hollow fiber maintaining a low pressure inside the capillary. Since the maximum length of traditional rigid fused silica fibers placed on a V-groove is typically limited by fabrication processes and handling, in 2008 Nagy et al. proposed the use of stretched flexible hollow fibers [32]. In the case of rigid glass fibers, the straightness of the capillary is determined by the fiber uniformity and by the quality of the support. Typical lengths are of the order of 1–1.5 m. On the contrary, the stretched flexible fibers with small wall thickness of the glass cladding do not pose such constraints on the fiber length, so that capillary with lengths of the order of a few meters can be used, without introducing losses related to the fiber curvature. Pulse compression using stretched fibers was reported in 2011 [33]. 71-fs pulses at 780-nm central wavelength and an energy of 1.1 mJ were injected into a 3-m-long stretched fiber filled with argon. After dispersion compensation by chirped mirrors, pulses as short as 4.5 fs were obtained with and energy of 0.42 mJ.

C. Compression of Circularly Polarized Pulses

A further increase of the maximum pulse energy can be obtained by using circularly polarized pulses, which lead to a reduction of both the Kerr nonlinearity [34] and ionization rate of the gas [35] compared to linearly polarized pulses at equivalent intensities. The physics of guided nonlinear propagation of ultrashort pulses with an arbitrary polarization state was investigated down to the few-cycle regime by Stagira and co-workers [36]. Pulses as short as 4.3 fs, with an energy of 1 mJ were reported by using the hollow fiber technique seeded with circularly polarized laser pulses [37]. A reported enhancement of 30% in energy throughput was observed when compared to the scenario involving linearly polarized laser input. Additionally, there was a notable improvement in the stability of the output spectral characteristics. As it will be discussed in Section VIII-B, circularly polarized pulses with duration of 6 fs, obtained by using the HCF technique, were used in 2001 to achieve the first clear experimental evidence of the role of the CEP in photoionization with few-cycle pulses [38].

D. TW-Scale HCF Compression

In general, the need to compress laser pulses with increasing energy has driven researchers to employ a combination of all the approaches described above. As early as 2014, Böhle et al. achieved a significant result: combining circularly polarized pulses in a 2-m-long stretched HCF with pressure gradient in helium, they demonstrated the production of 4-fs pulses with stable CEP and energy output of 3 mJ [39]. Through extensive engineering of the system, employing a fully vacuum-integrated post-compressor setup, Ouillé and colleagues have attained near-single-cycle pulse durations (3.4 fs or 1.5 cycles at a central wavelength of 719 nm) along with an energy output of 3.5 mJ [40]. These achievements have been accompanied by excellent beam quality and stable CEP. By employing an up-scaled version of this system, Nagy and colleagues have achieved the compression of 14-mJ, 50-fs pulses to a duration of 3.8 fs (corresponding to 1.5 optical cycles) with an output energy of 6.1 mJ and a peak power of 1.2 TW [41].

The use of long stretched HCFs has emerged as very interesting for compressing pulses generated by Yb-based laser systems. These systems exhibit promising characteristics for next-generation laser technology, including high power scaling, robustness, and compactness. Since the pulse duration of Yb lasers typically ranges from a few hundred femtoseconds to picoseconds, there is considerable interest in integrating Yb technologies with effective nonlinear pulse compression techniques. The main concept that has emerged in recent years for compressing pulses with durations of several hundred femtoseconds with high average power and/or high energy is to deliberately induce minimal spectral broadening per unit length over extended propagation distances. This experimental approach enables the achievement of spectral broadening primarily driven by SPM, consequently reducing the incidence of undesirable nonlinear effects that could potentially undermine spectral phase integrity and hinder the direct post-compression down to a single-cycle duration [42]. In 2019, a 30-fold compression of 5.8-mJ pulses with a duration of approximately 300 fs, produced by a Yb-fiber chirped pulse amplifier system operating at a repetition rate of 100 kHz, was demonstrated through the use of a 6-m-long HCF with an inner diameter of 400 μm and pressure gradient [43]. Notably, in this specific instance, gas pressures at both the input and output ends of the fiber were independently adjusted, resulting in the generation of 10-fs pulses at an average power of 318 W.

A record value in compressed pulse energy was reported by Fan et al. in 2021 [44] in the case of a high-energy Yb laser amplifier producing 70-mJ pulses with a duration of 230 fs. In this case, the experimental strategy employed to mitigate excessive gas ionization and prevent damage within the cladding of the HCF during the propagation of high-intensity laser pulses was the use of a large-core HCF. Indeed, as discussed by Vozzi et al. [22], a simple relationship between the minimum fiber radius, $a_{\min}$, and the energy, $\mathcal{E}_0$, and duration, T_0, of the input pulses can be derived by using numerical simulations of pulse propagation in gas-filled HCFs. This relationship is expressed as: $a_{\min} = AT_0^{-\alpha}\mathcal{E}_0^{\beta}$, where $\alpha \approx 0.45$, $\beta \approx 0.51$ and A is a constant, which depends on the gas. Employing a 2.8-m-long HCF with an inner diameter of 1 mm, Fan and colleagues reported on the generation of 25-fs pulses with an energy of 40 mJ, resulting in a record peak power of 1.3 TW [44].

IV. Supercontinuum Generation in HCFs

The production of pulses with duration below 4 fs requires the generation of ultra-broadband radiation. The HCF technique offers various possibilities to achieve this goal. In the following two experimental approaches will be discussed: (i) the implementation of two HCFs in a cascading geometry; (ii) the use of high pressure noble gases in a single fiber followed by a light-field synthesizer.

A. HCF Cascading

The use of two HCFs with a cascading geometry was proposed and implemented in 2002 [45]. A laser pulse was first injected into a gas-filled HCF and compressed through multiple reflections on chirped mirrors. The compressed pulses were then injected into a second gas-filled HCF, where supercontinuum generation was achieved. To experimentally demonstrate this spectral broadening technique, 25-fs pulses, with an energy of 0.5 mJ, were coupled into a 60-cm-long HCF, with an inner diameter of 0.5 mm, filled with argon. The argon pressure (0.2 bar) was adjusted in order to obtain pulses with duration of ~ 10 fs after compression. Only reflective optics were used at the output of the first fiber in order to reduce the dispersion. The compressed pulses were then injected into a second 60-cm-long hollow fiber, with an inner diameter of 0.3 mm, filled with argon with a pressure < 0.1 bar, thus obtaining a spectral broadening from ~ 400 nm to > 1 μm. Compared to the utilization of a single HCF, employing two fibers with an intermediate compression stage facilitates the generation of a supercontinuum exhibiting increased spectral energy within the blue and green segments of the spectrum. The energy of the output pulses was ~ 0.1 mJ, thus corresponding to a 20% total transmission efficiency of the complete setup. The group delay of the supercontinuum, measured by up-conversion with 25-fs, 800-nm pulses in a BBO crystal, was of the order of 600 fs from the near infrared to the blue components of the spectrum. The compression of the obtained supercontinuum down to the calculated transform-limited value (~ 1.9 fs), would require a control of the dispersion over a bandwidth exceeding 500 THz.

Ultrabroadband dispersion compensation was achieved by Schenkel et al. [46] by using a closed-loop combination of a spatial light modulator for adaptive pulse compression and spectral-phase interferometry for direct electric-field reconstruction (SPIDER) measurements as feedback signal. The measured temporal intensity gave a pulse duration of 3.8 fs, with a pulse energy of 15 μJ and a $\sim 270-$THz broad spectrum.

Voronin and co-workers [47] performed numerical simulations of pulse propagation in two cascaded HCFs, based on a proper modification of the generalized nonlinear Schrödinger [48], [49], including dispersion effects, Kerr nonlinearity, ionization-induced loss and nonlinearity and shock-wave effects. Input Gaussian pulses with 1-ps duration, central wavelength of 1030 nm and energy of 1.4 mJ were considered in the simulations. The fiber parameters used in the simulations were the following. (i) First fiber: length 2 m, inner diameter 285 μm, gas: xenon ($p = 1$ atm). (ii) Second fiber: length 3 m, inner diameter 360 μm, gas: argon ($p = 1.35$ atm). By considering a linear chirp compensation, pulses with duration close to the transform-limited value of ~ 2.8 fs could be generated, with a peak power of ~ 61 GW.

In 2016 two hollow fibers in cascaded configuration have been employed for the generation of sub-2-optical cycle pulses with 216-W average power [50]. The scalability of gas-filled HCFs for kW-level average power few-cycle lasers was first tested by using a cw single-mode fiber laser at a wavelength of 1070 nm, with an average power ranging from 8 to 1 kW [51]. The laser beam, characterized by an excellent spatial quality ($M^2 < 1.1$), was coupled in a 1-m-long hollow fiber with a 250-μm inner diameter, embedded into a V-groove made of aluminum, surrounded by a double-walled tube, constantly traversed by water. It was demonstrated that an efficient and stable coupling of 1-kW average power into the capillary is possible [51]. The setup was then used to compress high-average power 240-fs pulses generated by a fiber-chirped pulse amplification (FCPA) system which, upon employing coherent combination of 8 amplifier channels [52], delivers pulses with an average power up to 660 W at a repetition rate of 1.27 MHz, corresponding to a pulse energy of 520 μJ. A first pulse compression down to 30 fs was achieved by propagating the pulses in a 1-m-long HCF, with an inner diameter of 250 μm, placed on a water-cooled V-groove in a pressure chamber [51], and subsequent dispersion compensation with a chirped mirror compressor. The second compressor stage was formed by a 60-cm-long HCF, with an inner diameter of 250 μm, filled with neon at a pressure of 7.5 bar. Spectral broadening from 700 nm to 1250 nm was obtained. After compression in a second chirped mirror compressor a pulse duration of 6.3 fs was obtained, corresponding to less than 2 cycles at the central wavelength of 1030 nm. The average power was 216 W, corresponding to a pulse energy of 170 μJ.

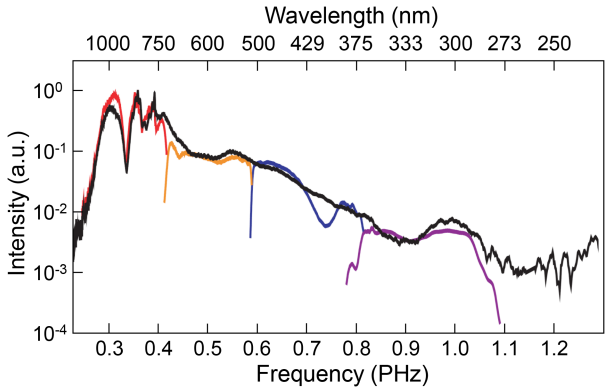

Fig. 3. Spectrum of the supercontinuum generated by propagation of 22-fs input pulses in a hollow fiber filled with neon at a pressure of 2.3 bar. Adapted from Ref. [55].

B. Light Field Synthesizer

In the case of pulses with duration of the order of 20 fs, also a single HCF allows one to achieve an ultrabroadband spectral broadening, as reported by Goulielmakis and coworkers [53], [54]. A coherent supercontinuum was generated by propagating 22-fs pulses at a central wavelength of 790 nm in a 1.1-m-long hollow fiber filled with neon at a pressure of ~ 2.3 bar [55]. The energy of the supercontinuum at the fiber exit was ~ 550 μJ. As a result of the propagation inside the hollow fiber the pulse spectrum spans more than two optical octaves, ranging from ~ 260 nm to ~ 1100 nm. Fig. 3 shows the pulse spectrum at the output of the fiber. Dispersion control over such a huge bandwidth cannot be achieved by using a simple chirped mirror compressor. In this case the compression of the output pulses was

obtained by employing the technique of coherent combination, or synthesis, of various pulses [56]. The beam at the output of the HCF was divided into four beams by dichroic beam-splitters, characterized by broad spectral bandwidths in four different spectral regions: in the DUV, from 270 to 350 nm; in the visible-ultraviolet (vis-UV), from 350 to 500 nm; in the visible (vis), from 500 to 700 nm and in the near infrared (NIR), from 700 to 1100 nm. The pulses in the four arms of the interferometer were subsequently compressed individually by multiple bounces on pairs of chirped mirrors, designed for the respective wavelength range, so that the pulses in the individual channels are compressed close to their bandwidth-limited durations. Since each set of chirped mirrors is used over a relatively narrow bandwidth (less than half an octave), almost standard design and fabrication techniques can be employed. Moreover, a pair of thin fused silica wedges was inserted in each channel, at the Brewster angle of each band to minimize losses, to finely tune the dispersion and the CEP of the pulses in the different channels. The pulse durations in the four channels of the synthesizer were measured to be ~ 6.5 fs in the DUV, ~ 6.5 fs in the vis-UV, ~ 7 fs in the visible and ~ 8.5 fs in the NIR. The total transmission of the synthesizer was $\sim 82\%$ of the energy of the input supercontinuum, so that the output pulse energy was ~ 320 μJ. The four pulses were then spatially and temporally superimposed in order to generate a single ultrabroadband pulse. The synthesis of light fields obtained by coherent superposition of various pulses requires a precise temporal and spatial overlap among the different pulses. Wavefront matching is required at any point along the propagation axis. Moreover, the optical path length in each arm of the field synthesizer must be perfectly stable. For this reason the experimental setup has been stabilized both passively and actively. The multi-arm interferometer has been realized as a quasi-monolithic setup; thermal stabilization was obtained by water flow through the volume of the baseplate. Moreover, an active stabilization scheme was additionally implemented. In order to measure the temporal characteristics of the generated pulses, the attosecond streaking technique was used [57]. Pulses as short as 380 as were measured [55].

V. HCF Compression in the IR Spectral Region

An important situation where the use of long HCFs can play a relevant role, is when the hollow fiber technique is applied to the compression of near- and mid-IR pulses. Indeed, the nonlinear refractive index of noble gases decreases upon increasing the wavelength [58]; for example in the case of argon $n_2(1800\,\text{nm}) = 0.59\ n_2(800\,\text{nm})$ [59]. In this case, in order to obtain a wide spectral broadening without increasing the gas pressure and the intensity, long capillaries can be used, as reported by Cardin et al. [60]. 11-mJ pulses, with a duration of 35 fs, produced by an optical parametric amplifier [61] at a central wavelength of 1.8 μm, were coupled into a stretched flexible fiber, with a 3-m length and an inner diameter of 1 mm, with a 300-μm-thick fused silica cladding surrounded by a polymer layer. A pressure gradient was used in the fiber. Spectral broadening ranging from 1.2 μm to 2.2 μm was achieved in argon (corresponding to a transform-limited pulse duration of 11.3 fs), with a maximum energy of 5 mJ. Dispersion compensation was obtained by propagation in a bulk medium [62], [63], [64]. Indeed, the negative GDD of bulk fused silica allows one to compensate for the positive dispersion introduced by propagation in the gas-filled HCF. Since the zero dispersion of fused silica is located at ~ 1.3 μm, it presents negative GDD throughout the whole spectral region of interest. By using a fused silica plate with correct thickness (between 2 and 4 mm), pulses as short as 12 fs, corresponding to two optical cycles, were obtained. Fine dispersion compensation was achieved by simply tilting the glass plate.

In 2016 the HCF technique has been applied to the compression of 85-fs, 5-mJ pulses, at a central wavelength of 3.2 μm, generated in a KTA parametric amplifier [65]. Passive CEP stabilization was obtained for the idler pulses at 3.2 μm. The pulses were injected into a 3-m long stretched fiber, with an inner diameter of 1 mm and a 300-μm-thick fused silica cladding, filled with argon with a pressure gradient scheme. Also in this case, dispersion compensation was achieved in a bulk medium. Pulses as short as 22 fs were measured after propagation in a 2-mm-thick CaF_2 window (at a 1.3-bar argon pressure at the fiber output), corresponding to a two-cycle pulse in the mid-IR, close to the transform-limited value. Various transparent materials in the mid-IR spectral region can be employed for dispersion compensation in a wide spectral range, such as calcium fluoride (CaF_2), magnesium fluoride (MgF_2), barium fluoride (BaF_2), sodium chloride (NaCl). BaF_2 and NaCl can be used for longer wavelengths ($> 4\,\mu$m). Due to the very short duration of the compressed pulses, the compensation of the third order dispersion (TOD) is critical. Note that all glasses exhibit positive TOD throughout their whole transmission range. As pointed out in Ref. [62], self-steepening due to propagation along the gas-filled fiber, induces a negative third-order component on the spectrally broadened pulse, which partially compensates for the positive TOD of the material.

As a final impressive result we mention the compression of 2.8-ps pulses with an energy of 45 mJ, generated by a 1-kHz repetition rate, Ho:YLF chirped pulse amplifier (wavelength 2.05 μm) [66]. The compression was obtained by using a two-stage configuration. In the first stage pulse spectral broadening was obtained by focusing the laser pulses in air, at a focused intensity close to the onset of filamentation. Compression to 1.4 ps was achieved by using a single-pass grating compressor (with an overall transmission of the first compressor stage of $\sim 82\%$). The second stage was composed by a stretched 3-m-long HCF with an inner diameter of 500 μm, operated with a pressure gradient (krypton gas was employed). Active cooling was implemented to manage the heating effects induced by an average power of approximately 35 W at the input. After dispersion compensation with a set of chirped mirrors, pulses as short as 86 fs were measured with an energy of 20.8 mJ, corresponding to a peak power of 0.2 TW.

VI. Few-Cycle Pulses in the UV Spectral Region

The generation of few-femtoseconds laser pulses in the DUV-UV spectral region is crucial for probing the ultrafast electron

dynamics in molecules with biological and opto-electronic interest, particularly those featuring electronic absorption bands within this specific spectral range [67].

In 1999, Durfee et al. demonstrated the generation of 8-fs pulses at 270 nm through cross-phase modulation in gas-filled HCFs [68]. By injecting the fundamental and second harmonic of a femtosecond laser into a HCF filled with argon, pulses at the third harmonic (TH) were generated via parametric frequency mixing ($3\omega = 2\omega + 2\omega - \omega$) under phase-matching conditions, achieving approximately $30\% - 40\%$ conversion efficiency from the pump light at 2ω [69]. The interaction of self- and cross-phase modulation induced significant spectral broadening of the idler pulse at 3ω. Dispersion compensation was achieved by using a grating compressor in single-pass configuration, with a throughput of 50%. Pulses as short as 8 fs have been measured by self-diffraction frequency-resolved optical gating (SD-FROG) [70], [71]. Compressed pulse energy was greater than 1 μJ.

Tzankov and coworkers extended the use of four-wave difference-frequency mixing (FWDFM) in gas-filled HCF for the generation of the fifth harmonic (FH) of femtosecond pulses produced by a Ti:sapphire laser [72]. In this case two pump photons at the TH (3ω) were mixed with an idler photon at the fundamental frequency (ω, corresponding to a wavelength of 805 nm), thus giving rise to the generation of the FH ($5\omega = 3\omega + 3\omega - \omega$) at 161 nm. The TH and fundamental pulses were coupled in an argon-filled HCF and the generated FH was selected with a dichroic mirror. Coupling both pump and idler pulses into the fundamental EH $_{11}$ mode of the HCF and properly adjusting the argon pressure to achieve phase-matching, pulses at the FH were produced with an energy of $\sim$50 nJ. Very recently the generation of 37-fs pulses at the FH of Ti:sapphire with an energy of 4 μ J has been reported, corresponding to a $\sim 10\%$ conversion efficiency from the TH pump pulse [73]. Also in this case the FH pulses are produced employing FWDFM in a helium-filled HCF by using TH pump pulses and fundamental idler pulses. The positive dispersion of the gas is balanced by the negative contribution of the waveguide propagation in the HCF at the phase-matching pressure.

Few-femtosecond UV pulses with energy in the microjoule range can be generated by employing cross-phase modulation (XPM) between an intense NIR pulse and its TH, co-propagating in a gas-filled HCF. In XPM an intense pulse traveling through a Kerr medium induces changes in the optical phase of a second pulse, typically weaker and of a different wavelength. Jiang et al. conducted experimental and numerical investigations on the utilization of XPM within a neon-filled HCF to spectrally tune, broaden, and compress UV pulses using an intense NIR pulse and its TH. They achieved the generation of UV pulses with durations as short as 6 fs and energies exceeding 10 μJ [74].

The HCF technique was also applied to compress high-energy 110-fs pulses generated by a hybrid Ti:sapphire-KrF excimer laser system operating at 248.5 nm [75]. In this case a 2-m-long stretched HCF was used with an inner diameter of 320 μJ, filled with neon in pressure gradient configuration. After dispersion compensation by using a single-pass grating compressor, pulses as short as 24 fs were generated with an energy of 200 μJ.

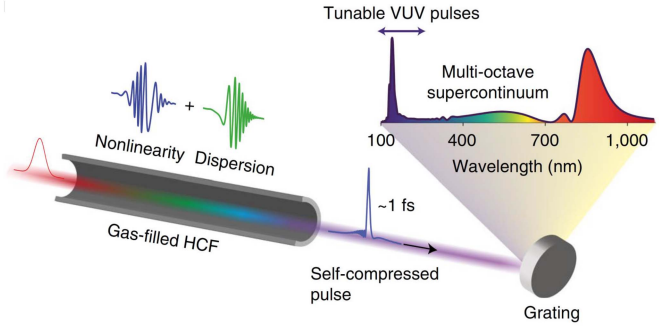

Fig. 4. Soliton dynamics in a gas-filled HCF, wherein the interplay of nonlinearity and dispersion leads directly to extreme self-compression, UV emission, and the generation of a multi-octave supercontinuum (from Ref. [76]).

Temporal characterization was performed by using an all-reflective single-shot transient grating FROG setup.

In 2019, Travers and colleagues reported on a novel experimental technique for efficient generation of ultrashort pulses with tunability across an ultrabroad spectral range. This approach relies on the utilization of RDW emission in gas-filled HCFs [76]. The achieved ultrashort and tunable pulses exhibited energy levels in the microjoule range, representing a substantial enhancement of up to three orders of magnitude compared to the energy obtained through RDW emission in gas-filled anti-resonant photonic crystal fibers [77]. RDW emission, also referred to as non-solitonic or Čerenkov radiation, is a phenomenon occurring when a fraction of the energy within a self-compressing soliton, propagating through a fiber, is transferred to a secondary pulse at a phase-matched shifted frequency, in the presence of higher-order dispersive effects [78], [79], [80], [81]. In the conventional HCF compression approach, the fiber dynamics are predominantly influenced by nonlinear spectral broadening mechanisms, in particular SPM and self-steepening, and the anomalous dispersion required for pulse compression is achieved by using chirped mirrors. In contrast, the adoption of soliton dynamics in a gas-filled HCF represents a paradigm shift, visually illustrated in Fig. 4. In this case, the interplay of both nonlinearity and dispersion directly leads to pronounced self-compression effects, accompanied by the generation of UV emission and the formation of a multi-octave supercontinuum.

In 2023 Reduzzi et al. reported on the first complete temporal characterization of sub-3-fs pulses generated by RDW emission in HCFs, spectrally tunable in a broad DUV/UV spectral region [82]. Pulses with a duration of 9.7 fs, generated by a hollow fiber compressor, were coupled into a 60-cm-long HCF with an inner diameter of 150 μm to induce RDW emission. To facilitate nearly dispersion-free transmission of RDW pulses into a vacuum system, a gradual reduction in longitudinal gas pressure along the fiber was implemented, as described in [83]. This is particularly important in the DUV/UV spectral region given the high dispersion characteristics of air, which is $\sim$ 80 fs^2/m at 300 nm. Compounding this issue is the unavailability of broadband dispersion compensation methods within this specific spectral range.

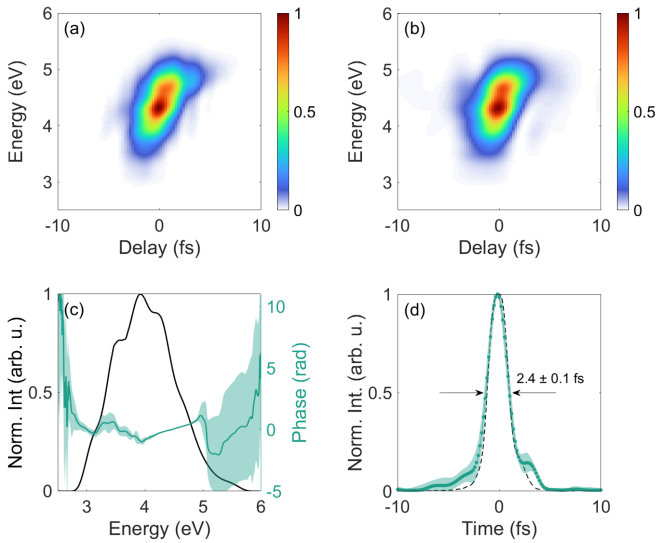

Fig. 5. Experimental (a) and retrieved (b) SD-FROG spectrograms of the RDW pulses generated in neon. (c) Experimental spectrum (black line) and reconstructed spectral phase (green line) of the RDW pulse. (d) The dotted green curve represents the retrieved temporal intensity profile of the RDW pulse; the black dashed curve is the intensity profile calculated by using numerical simulations. Both in (c) and (d) the shaded green area represents the standard deviation obtained by comparing a set of 10 reconstructions (from Ref. [82]).

Temporal characterization was achieved by using an all-in-vacuum SD-FROG experimental apparatus [70], [71]. Fig. 5(a) shows the experimental SD-FROG spectrogram of the RDW pulses generated in neon. Fig. 5(b) shows the retrieved SD-FROG spectrogram, in excellent agreement with the experimental spectrogram. Fig. 5(c) and (d) show the retrieved spectral phase and temporal intensity profile, respectively, of the RDW pulse. A duration of 2.4 ± 0.1 fs (FWHM) was obtained (to be compared to a transform-limited duration of 1.9 fs). Remarkably, the retrieved temporal pulse shape was in excellent agreement with the one obtained from numerical simulations, shown as dashed line in Fig. 5(d).

VII. HCFs and Molecular Gases

In this section we will mention the use of molecular gases in HCFs for spectral broadening and pulse compression. The overall nonlinear response of a gas consists of two main components: instantaneous and delayed. The instantaneous part corresponds to the nonlinear distortion of the electron cloud surrounding atoms or molecules, known as electronic response. The delayed component involves field-induced molecular rotation and vibration. Together, these elements are collectively referred to as the optical Kerr nonlinearity. In the case of molecular gases, the response due to the alignment and stretching of the molecular bonds in the intense laser field can be the dominant contribution. This response can be described by a time-domain Raman response function $R(t)$. The total nonlinear index of refraction,to first order in the laser intensity, can be written as [84]

$$\Delta n(t) = n_2 I(t) + \int_{-\infty}^{\infty} R(t-t')I(t')\,dt', \qquad (3)$$

where $I(t)$ is the laser intensity.

Spectral broadening of 140-fs pulses in a hollow fiber filled with nitrogen was first reported by Nisoli et al. in 1997 [85]. The generated spectra exhibited pronounced amplitude modulations characteristic of a pure SPM process, along with a distinct red shift indicative of a noninstantaneous Kerr response within the medium [86], [87]. A nonlinearity response time of $\sim$240 fs was estimated by using numerical simulations. In contrast, when employing 20-fs input pulses, a distinct scenario emerged. Spectral broadening with less prominent modulations was measured in this case, with a less evident cutoff in the blue side. In the presence of very short optical pulses, the instantaneous electronic contribution to the nonlinear index dominates.

More recently Beetar et al. reported on the generation of a multioctave supercontinuum by propagation in a hollow fiber filled with molecular gases of relatively long pulses for which the rotational nonlinearity can be assumed as nearly instantaneous [88]. By selecting the molecular gas in accordance with the input pulse duration, it was possible to achieve a more than tenfold enhancement in the total nonlinearity compared to an atomic gas with similar nonlinear susceptibility and ionization potential. Beetar and colleagues investigated the application of 80-cycle pulses from an industrial-grade laser amplifier. These pulses were employed to drive both molecular alignment and supercontinuum generation within a gas-filled capillary. This process resulted in the production of more than two octaves of coherent bandwidth and an impressive $> 45-$fold compression down to a duration of 1.6 cycles. The exploitation of the enhanced nonlinearity linked to rotational motion offers opportunities for applications in long-wavelength frequency conversion and the compression of picosecond lasers.

The generation of multidimensional solitary states (MDSS) in HCFs filled with nitrogen was reported by Safaei et al. [89]. The self-trapped MDSS generated in the initial segment of the fiber experiences an enhanced Raman cascading process along the extended interaction length of the HCF. This leads to the generation of broadband spectra that are redshifted at the output of the fiber. Notably, the output MDSS pulses exhibit an unexpected negative quadratic spectral phase. This stands in contrast to the spectral phase acquired through spectral broadening relying on Kerr nonlinearity. The idea at the heart of the method is displayed in Fig. 6(a). Briefly, the input laser beam is coupled to the fundamental, linearly polarized mode (LP_{01}) of a HCF filled with a molecular gas (nitrogen). In the high-energy regime, multiple higher-order linearly polarized modes (LP_{0n}) are generated at the beginning of the fiber, which determine an enhancement of the Raman process in the molecular gas. This, in turn, leads to a self-trapping mechanism of the laser beam inside the fiber, with the generation of MDSS. The combination of self-trapping and very low modal dispersion of the large-core fiber, results in a strong red-shift and spectral broadening of the laser pulses through cascaded stimulated Raman scattering (SRS), as shown in Fig. 6(b).

VIII. First Applications of Pulses Produced by the HCF Compression Technique

The first application of 10-fs pulses produced by a HCF compressor was the investigation of the temporal evolution

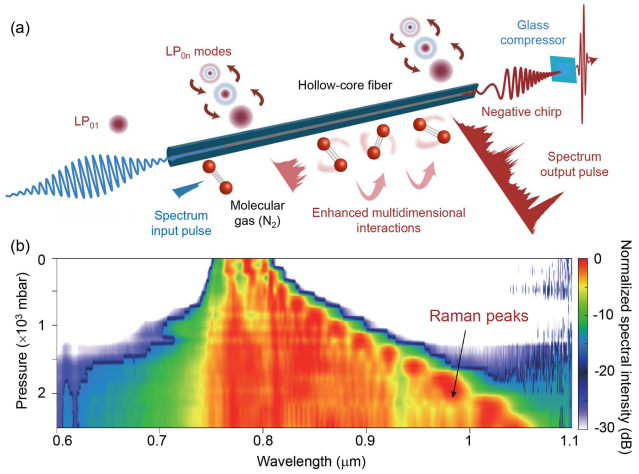

Fig. 6. (a) Conceptual scheme of the MDSS generation in a HCF filled with nitrogen, with red-shift and spectral broadening by stimulated Raman Scattering (SRS) and subsequent pulse compression by propagation in a window of fused silica. (b) Experimental spectral broadening of a 700-fs input pulse, with central wavelength of 780 nm, 5-mJ energy, after propagation in a 3-m-long HCF with an inner diameter of 500 μm, filled with N_2 for increasing gas pressure. Adapted from [89].

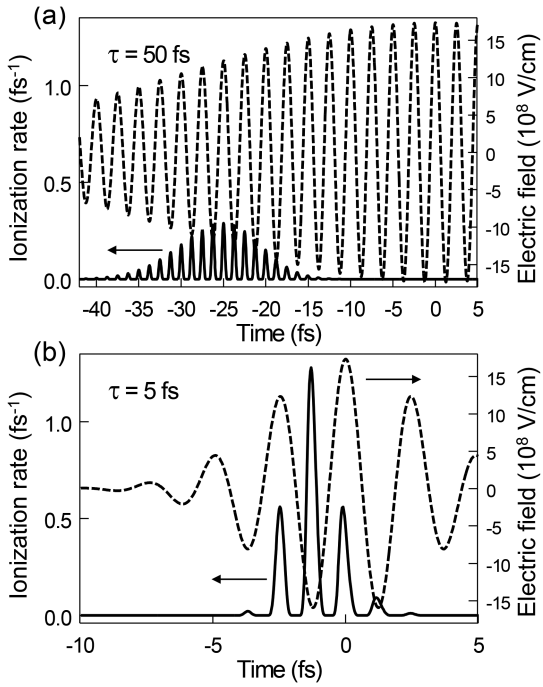

Fig. 7. Instantaneous ionization rate (solid lines) of helium produced by a linearly polarized electric field (dashed lines) of a laser pulse with central wavelength $\lambda = 800$ nm, a peak intensity $I = 4 \times 10^{15}$ W/cm^2 and pulse duration $\tau = 50$ fs (a) and $\tau = 5$ fs (b).

of single-electron wave packets following femtosecond laser excitation in the KBr F center [90]. The electron dynamics induced subpicosecond periodic oscillations in the sample transmission, effectively monitored in real-time through pump-probe techniques. This approach directly revealed the vibrational frequencies corresponding to localized modes associated with both ground and excited electronic states. The time-resolved investigation unequivocally illustrated the robust coupling between the optical transition of the color center electron and the localized A_{1g} breathing mode of the lattice.

A. *Generation of Isolated Attosecond Pulses*

The first application to extreme nonlinear optics of high-energy 5-fs pulses produced by using this compression technique was reported in 1997 by Spielmann et al. [91], with the generation of coherent EUV radiation extending to wavelengths below the carbon K edge at 4.37 nm. This was obtained by focusing 5-fs pulses into a helium gas jet, resulting in the generation of coherent and well-collimated EUV beam extending well into the water window. Due to the exceedingly rapid rise time of the driving pulses, neutral atoms can experience high fields before undergoing depletion through ionization, thus increasing the maximum photon energy of the EUV radiation produced by high-order harmonic generation [3]. Indeed, when a femtosecond laser pulse characterized by high peak power is focused onto a gaseous medium at intensities ranging from 10^{13} to 10^{14} W/cm^2, the transmitted radiation spectrum exhibits components at frequencies that are multiples of the fundamental frequency. The spectral amplitude of these harmonics displays a distinct decline, particularly from the third to approximately the fifth harmonic. Subsequently, a plateau region is observed, initially identified by L'Huillier and colleagues [92], where the intensities of the harmonics remain relatively constant up to a maximum photon energy, $\hbar\omega_c$, defined by the cutoff law [93]. This law is expressed as $\hbar\omega_c \approx I_p + 3.17U_p$, where I_p represents the ionization potential of the gas and $U_p \propto I\lambda^2$ is the ponderomotive potential (i.e., the mean kinetic energy of an electron oscillating in the laser field). Here, I and λ represent the peak intensity and central wavelength of the driving pulse, respectively. Beyond this defined photon energy, a notable decrease in generation efficiency ensues. The cutoff law may suggest the possibility of indefinitely increasing the cutoff photon energy by increasing the driving intensity; however, this is an inaccurate assumption. The quantum nature of light emission through recombination imposes intrinsic limitations. The generation of EUV radiation involves the superposition of the returning electron wave and the ground state electron wave [3]. It is crucial that the ground-state population is not entirely depleted when the liberated electron wave recombines. For a pulse laser field, the ground-state population can be fully depleted by a portion of the leading edge, leaving no population available for the peak portion of the laser pulse. Consequently, for a specific atom type, there exists a maximum laser intensity that the ground state can withstand, known as the saturation intensity (I_s). When the depletion of the ground-state population by ionization is taken into account, the cutoff law becomes:

$$\hbar\omega_c = I_p + 3.17U_p(I_s) \tag{4}$$

As evidenced by Brabec [94], in the multi-cycle regime there is an accumulation of ionized target atoms over numerous optical cycles. Fig. 7 displays the instantaneous ionization rates (solid lines) produced by 50-fs (Fig. 7(a)) and 5-fs (Fig. 7(b)) pulses

focused in helium with a peak intensity $I = 4 \times 10^{15}$ W/cm^2. As clearly shown in the figure, the depletion of the ground state occurs well in advance of the peak of the laser pulse in the multi-cycle case. In the case of few-cycle pulses, the saturation of ionization is shifted to significantly higher intensities. The shorter is the driving pulse, the stronger is the laser field the electron experiences at the instant of its detachment from the atom.

An additional highly significant benefit provided by employing intense few-cycle pulses in high-order harmonic generation is the ability to confine the EUV emission to a single event by implementing different gating techniques [95]. The first experimental demonstration of the generation of isolated attosecond pulses was reported by Hentschel et al. in 2001 [96], by spectral selection of the cutoff portion of the EUV spectrum generated by using 7-fs driving pulses produced through the HCF compression technique, resulting in the generation of isolated attosecond pulses with a duration of 650 ± 150 as. Isolated attosecond pulses can be produced by using temporal gating techniques. In this case the confinement of the EUV generation to a single emission event is achieved through temporal modulation of a specific property of the driving electric field. Importantly, this modulation possesses the potential for implementation without constraints on the bandwidth of the resulting EUV pulse [95]. The most common temporal gating techniques, which have been experimentally demonstrated for the generation of isolated attosecond pulses are the polarization gating [97], [98] and the ionization gating [99] techniques. Both methodologies derive enhanced efficacy from the utilization of high-energy few-cycle driving pulses [100].

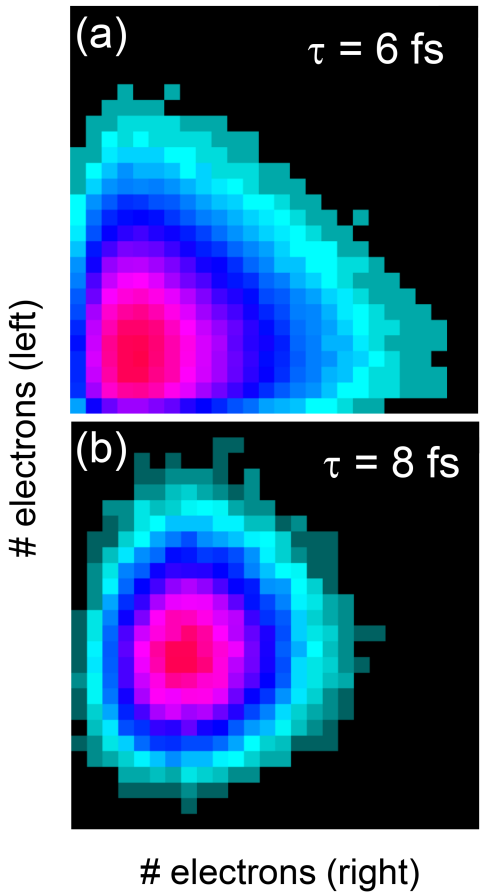

Fig. 8. Contingency maps resulted for (a) 6-fs and (b) 8-fs pulse duration. The measurements were obtained by focusing on a krypton jet circularly polarized laser pulses with peak intensity $I = 5 \times 10^{13}$ W/cm^2.

B. Strong-Field Ionization by Few-Cycle Pulses

In the case of few-cycle pulses the CEP governs the temporal evolution of the laser electric field. As numerous effects in intense-field atom interaction rely on the temporal characteristics of the electric field, the CEP assumes significance in various nonlinear processes. One notable example is the process of photoionization, which is at the heart of the generation of attosecond pulses. The photoionization of atoms in intense laser fields is characterized by above-threshold ionization (ATI) [101]. ATI means that an atom may absorb more photons than are necessary for its ionization. This leads to photoelectron energies considerably higher than the photon energy. For a few-cycle laser pulse, depending on the CEP, the temporal variation of the electric field becomes asymmetric. Accordingly, the emission of photoelectrons loses inversion symmetry, i.e. a left-right asymmetry appears. Depending on the CEP the maximum of the field points to the left or to the right. Consequently, nonlinear photoionization of atoms will exhibit a preference for either leftward or rightward emission based on the CEP. This translates into an anticorrelation in the number of electrons emitted in opposite directions.

In 2001 Paulus et al. reported on the first experimental evidence of the role of CEP of few-cycle pulses in photoionization [38]. The basic idea of the experiment was to place two electron detectors in opposite directions with respect to the laser focus. In particular, the influence of the CEP was investigated by using 6-fs, circularly polarized pulses focused onto a krypton jet. The amplitude of the electric field for this kind of pulses varies continuously from zero at the peak and back to zero with the field vector rotating at the laser frequency. For each laser pulse, the number of electrons detected with both detectors was recorded. Each laser pulse was characterized by two numbers: namely, the number of electrons detected in the left-hand and that in the right-hand arm of the ATI spectrometer. These pairs of numbers can be interpreted as coordinate in a contingency map. The signature of an effect from the CEP is an anticorrelation in the number of detected photoelectrons, which gives rise to a structure inclined at -45° clearly visible in the contingency map shown in Fig. 8(a) in the case of 6-fs driving pulses. By using 8-fs driving pulses the measured contingency map, shown in Fig. 8(b) does not show any clear evidence of anticorrelation.

As a final example of one of the first applications of the compressed pulses to strong-field ionization, we mention the investigation of the ATI process at the few-cycle limit [102]. For linear laser polarization, the appearance of ATI spectra presents an initial steep decrease in electron photon yield for the first few orders followed by a plateau-like structure, i.e. a more or less constant yield over an extended energy range. The ATI

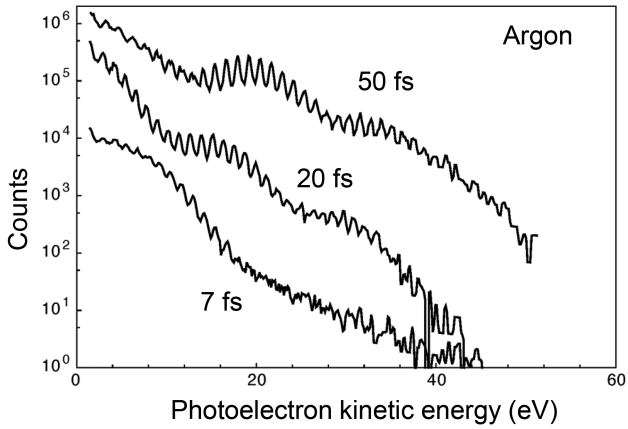

Fig. 9. ATI spectra in argon recorded for different pulse duration. The ATI plateau, which is due to scattering during the ionization process, is weaker for shorter pulse duration. The spectra are separated in the vertical direction for visual convenience.

plateau has been explained as being due to electrons returning to the ion core during the ionization process and rescattering elastically there. The plateaus end with a steep roll-off, the so-called ATI-cutoff. These spectra closely resembles those of HHG: the major difference is that in ATI the spectra are not hindered by the fact that propagation plays a major role, since they originate from single-atom effect. Using few-cycle laser pulses, ATI spectra allow to study processes originating from a single optical cycle. For longer pulses, in contrast, many optical cycles can contribute and strongly alter the appearance of spectra. By using sub-10-fs pulses produced by the hollow fiber compression technique, Grasbon et al. demonstrated that the ATI plateau exists also for few-cycle laser pulses. However, it was observed that the plateau is less pronounced in comparison to results obtained with multi-cycle excitation pulses, as shown in Fig. 9, which displays the ATI spectra in argon recorded for different pulse durations. This can be traced back to the absence of resonance-like effects due to constructive interference of electron wave-packets that return several times to the ion core during the ionization process [103].

IX. Conclusion

Nearly three decades since its initial demonstration, the HCF compression technique remains a prominent method widely employed in numerous laboratories, with ongoing reports of new experimental implementations. This technique has proven its efficacy in generating few-cycle pulses with millijoule-level energy and central wavelengths spanning from the UV to the mid-IR spectral regions. By facilitating the production of ultrashort pulses across a broad spectrum, this technique has significantly advanced research capabilities, enabling breakthroughs in the exploration of ultrafast processes and phenomena. The impact of the hollow fiber compression technique on attosecond science has been pivotal. In particular, it has played a crucial role in both the generation and application of isolated attosecond pulses. The HCF compression technique not only maintains its relevance but also continues to inspire new avenues of research and innovation. Its consistent use in laboratories and the generation of novel experimental implementations highlight its staying power as a vital tool for advancing our understanding of ultrafast processes. Future research may focus on extending the spectral coverage of the HCF compression technique. Expanding the wavelength range, possibly into EUV or longer mid-IR wavelengths, could open new avenues for scientific investigations and technological applications in fields such as spectroscopy, imaging, and materials science.

References

[1] H. Fattahi et al., "Third-generation femtosecond technology," *Optica*, vol. 1, pp. 45–63, 2014.
[2] F. Krausz and M. Ivanov, "Attosecond physics," *Rev. Modern Phys.*, vol. 81, pp. 163–234, 2009.
[3] M. Nisoli, P. Decleva, F. Calegari, A. Palacios, and F. Martín, "Attosecond electron dynamics in molecules," *Chem Rev.*, vol. 117, pp. 10760–10825, 2017.
[4] R. Borrego-Varillas, M. Lucchini, and M. Nisoli, "Attosecond spectroscopy for the investigation of ultrafast dynamics in atomic,molecular and solid-state physics," *Rep. Prog. Phys.*, vol. 85, 2022, Art. no. 066401.
[5] G. Mourou, T. Tajima, and S. V. Bulanov, "Optics in the relativistic regime," *Rev. Mod. Phys.*, vol. 78, pp. 309–371, 2006.
[6] A. Dubietis and G. Jonušauskas, and A. Piskarskas, "Powerful femtosecond pulse generation by chirped and stretched pulse parametric amplification in BBO crystal," *Opt. Commun.*, vol. 88, pp. 437–440, 1992.
[7] M. Nisoli, S. De Silvestri, and O. Svelto, "Generation of high-energy 10-fs pulses by a new pulse compression technique," *Appl. Phys. Lett.*, vol. 68, pp. 2793–2795, 1996.
[8] T. Nagy, P. Simon, and L. Veisz, "High-energy few-cycle pulses: Post-compression techniques," *Adv. Phys.: X*, vol. 6, 2021, Art. no. 1845795.
[9] A.-L. Viotti et al., "Multi-pass cells for post-compression of ultrashort laser pulses," *Optica*, vol. 9, pp. 197–216, 2022.
[10] F. Gires and P. Tournois, "An interferometer useful for pulse compression," *C. R. Acad. Sci. Paris*, vol. 258, pp. 6112–6115, 1964.
[11] J. Giordmaine, M. Duguay, and J. Hansen, "Compression of optical pulses," *IEEE J. Quantum Electron.*, vol. 4, pp. 252–255, May 1968.
[12] R. A. Fisher, P. L. Kelley, and T. K. Gustafson, "Subpicosend pulse generation using the optical kerr effect," *Appl. Phys. Lett.*, vol. 14, pp. 140–143, 1969.
[13] E. P. Ippen, C. V. Shank, and T. K. Gustafson, "Self–phase modulation of picosecond pulses in optical fibers," *Appl. Phys. Lett.*, vol. 24, pp. 190–192, 1974.
[14] R. H. Stolen and C. Lin, "Self-phase-modulation in silica optical fibers," *Phys. Rev. A*, vol. 17, pp. 1448–1453, 1978.
[15] H. Nakatsuka, D. Grischkowsky, and A. C. Balant, "Nonlinear picosecond-pulse propagation through optical fibers with positive group velocity dispersion," *Phys. Rev. Lett.*, vol. 47, pp. 910–913, 1981.
[16] C. Rolland and P. B. Corkum, "Compression of high-power optical pulses," *J. Opt. Soc. Amer. B*, vol. 5, pp. 641–647, 1988.
[17] A. Braun et al., "Self-channeling of high-peak-power femtosecond laser pulses in air," *Opt. Lett.*, vol. 20, pp. 73–75, 1995.
[18] P. B. Corkum, C. Rolland, and T. Srinivasan-Rao, "Supercontinuum generation in gases," *Phys. Rev. Lett.*, vol. 57, pp. 2268–2271, 1986.
[19] E. Marcatili and R. Schmeltzer, "Hollow metallic and dielectric waveguide for long distance optical transmission and laser," *Bell Syst. Tech. J.*, vol. 43, pp. 1783–1809, 1964.
[20] M. Nisoli et al., "Compression of high-energy laser pulses below 5 FS," *Opt. Lett.*, vol. 22, pp. 522–524, 1997.
[21] G. Cerullo et al., "Few-optical-cycle laser pulses: From high peak power to frequency tunability," *IEEE J. Sel. Topics Quantum Electron.*, vol. 6, pp. 948–958, Nov./Dec. 2000.
[22] C. Vozzi, M. Nisoli, G. Sansone, S. Stagira, and S. De Silvestri, "Optimal spectral broadening in hollow-fiber compressor systems," *Appl. Phys. B*, vol. 80, pp. 285–289, 2005.
[23] N. Milosevic, G. Tempea, and T. Brabec, "Optical pulse compression: Bulk media versus hollow waveguides," *Opt. Lett.*, vol. 25, pp. 672–674, 2000.

[24] D. Wang, Y. Leng, and Z. Huang, "Divided-pulse compression with gas-filled hollow-core fiber for generation of high-energy few-cycle pulses," *J. Opt. Soc. Amer. B*, vol. 31, pp. 1248–1254, 2014.

[25] F. Guichard et al., "Energy scaling of a nonlinear compression setup using passive coherent combining," *Opt. Lett.*, vol. 38, pp. 4437–4440, 2013.

[26] A. Klenke et al., "Divided-pulse nonlinear compression," *Opt. Lett.*, vol. 38, pp. 4593–4596, 2013.

[27] H. Jacqmin et al., "Passive coherent combining of CEP-stable few-cycle pulses from a temporally divided hollow fiber compressor," *Opt. Lett.*, vol. 40, pp. 709–712, 2015.

[28] A. Suda, M. Hatayama, K. Nagasaka, and K. Midorikawa, "Generation of sub-10-fs, 5-mJ-optical pulses using a hollow fiber with a pressure gradient," *Appl. Phys. Lett.*, vol. 86, 2005, Art. no. 111116.

[29] M. Nurhuda et al., "Propagation dynamics of femtosecond laser pulses in a hollow fiber filled with argon: Constant gas pressure versus differential gas pressure," *J. Opt. Soc. Amer. B*, vol. 20, pp. 2002–2011, 2003.

[30] M. Nurhuda, A. Suda, M. Kaku, and K. Midorikawa, "Optimization of hollow fiber pulse compression using pressure gradients," *Appl. Phys. B*, vol. 89, pp. 209–215, 2007.

[31] S. Bohman, A. Suda, T. Kanai, S. Yamaguchi, and K. Midorikawa, "Generation of 5.0 fs, 5.0 mJ pulses at 1 kHz using the hollow-fiber pulse compression," *Opt. Lett.*, vol. 35, pp. 1887–1889, 2010.

[32] T. Nagy, M. Forster, and P. Simon, "Flexible hollow fiber for pulse compressors," *Appl. Opt.*, vol. 47, pp. 3264–3268, 2008.

[33] T. Nagy, V. Pervak, and P. Simon, "Optimal pulse compression in long hollow fibers," *Opt. Lett.*, vol. 36, pp. 4422–4424, 2011.

[34] R. W. Boyd, *Nonlinear Optics*, Cambridge, MA, USA: Academic, 2003.

[35] S. Petit, A. Talebpour, A. Proulx, and S. L. Chin, "Polarization dependence of the propagation of intense laser pulses in air," *Opt. Commun.*, vol. 175, pp. 323–327, 2000.

[36] S. Stagira et al., "Nonlinear guided propagation of few-optical-cycle laser pulses with arbitrary polarization states," *Phys. Rev. A*, vol. 66, 2002, Art. no. 033810.

[37] X. Chen et al., "Generation of 4.3 fs, 1 mJ laser pulses via compression of circularly polarized pulses in a gas-filled hollow-core fiber," *Opt. Lett.*, vol. 34, pp. 1588–1590, 2009.

[38] G. G. Paulus et al., "Absolute-phase phenomena in photoionization with few-cycle laser pulses," *Nature*, vol. 414, pp. 182–184, 2001.

[39] F. Böhle et al., "Compression of CEP-stable multi-mj laser pulses down to 4 fs in long hollow fibers," *Laser Phys. Lett.*, vol. 11, 2014, Art. no. 095401.

[40] M. Ouillé et al., "Relativistic-intensity near-single-cycle light waveforms at kHz repetition rate," *Light: Sci. Appl.*, vol. vol. 9, 2020, Art. no. 47.

[41] T. Nagy, M. Kretschmar, M. J. J. Vrakking, and A. Rouzee, "Generation of above-terawatt 1.5-cycle visible pulses at 1 kHz by post-compression in a hollow fiber," *Opt. Lett.*, vol. 45, pp. 3313–3316, 2020.

[42] Y.-G. Jeong et al., "Direct compression of 170-fs 50-cycle pulses down to 1.5 cycles with 70% transmission," *Sci. Rep.*, vol. 8, 2018, Art. no. 11794.

[43] T. Nagy et al., "Generation of three-cycle multi-millijoule laser pulses at 318 w. average power," *Optica*, vol. 6, pp. 1423–1424, 2019.

[44] G. Fan et al., "70 mJ nonlinear compression and scaling route for an yb amplifier using large-core hollow fibers," *Opt. Lett.*, vol. 46, pp. 896–899, 2021.

[45] M. Nisoli et al., "Ultra-broadband continuum generation by hollow-fiber cascading," *Appl. Phys. B*, vol. 75, pp. 601–604, 2002.

[46] B. Schenkel et al., "Generation of 3.8-fs pulses from adaptive compression of a cascaded hollow fiber supercontinuum," *Opt. Lett.*, vol. 28, pp. 1987–1989, 2003.

[47] A. A. Voronin, J. M. Mikhailova, M. Gorjan, Z. Major, and A. M. Zheltikov, "Pulse compression to subcycle field waveforms with split-dispersion cascaded hollow fibers," *Opt. Lett.*, vol. 21, pp. 4354–4357, 2013.

[48] L. Bergé, S. Skupin, R. Nuter, J. Kasparian, and J.-P. Wolf, "Ultrashort filaments of light in weakly ionized, optically transparent media," *Rep. Prog. Phys.*, vol. 70, 2007, Art. no. 1633.

[49] A. Couairon and A. Mysyrowicz, "Femtosecond filamentation in transparent media," *Phys. Rep.*, vol. 441, pp. 47–189, 2007.

[50] S. Hädrich et al., "Energetic sub-2-cycle laser with 216-W average power," *Opt. Lett.*, vol. 41, pp. 4332–4335, 2016.

[51] S. Hädrich et al., "Scalability of components for kW-level average power few-cycle lasers," *Appl. Opt.*, vol. 55, pp. 1636–1640, 2016.

[52] M. Müller et al., "1 kW 1 mJ eight-channel ultrafast fiber laser," *Opt. Lett.*, vol. 41, pp. 3439–3442, 2016.

[53] A. Wirth et al., "Synthesized light transients," *Science*, vol. 334, pp. 195–200, 2011.

[54] M. Th Hassan et al., "Attosecond photonics: Synthesis and control of light transients," *Rev. Sci. Instrum.*, vol. 83, 2012, Art. no. 1111301.

[55] M. Th Hassan et al., "Optical attosecond pulses and tracking the nonlinear response of bound electrons," *Nature*, vol. 530, pp. 66–70, 2016.

[56] C. Manzoni et al., "Coherent pulse synthesis: Towards sub-cycle optical waveforms," *Laser Photon. Rev.*, vol. 9, pp. 1863–1899, 2015.

[57] E. Goulielmakis et al., "Direct measurement of light waves," *Science*, vol. 305, pp. 1267–1269, 2004.

[58] W. Ettoumi, Y. Petit, J. Kasparian, and J.-P. Wolf, "Generalized miller formulæ," *Opt. Exp.*, vol. 18, pp. 6613–6620, 2010.

[59] D. Wang, Y. Leng, and Z. Xu, "Measurement of nonlinear refractive index coefficient of inert gases with hollow-core fiber," *Appl. Phys. B*, vol. 111, pp. 447–452, 2013.

[60] V. Cardin et al., "0.42 TW 2-cycle pulses at 1.8 μm via hollow-core fiber compression," *Appl. Phys. Lett.*, vol. 107, 2015, Art. no. 181101.

[61] N. Thiré et al., "10 mJ 5-cycle pulses at 1.8 μm through optical parametric amplification," *Appl. Phys. Lett.*, vol. 106, 2015, Art. no. 091110.

[62] B. E. Schmidt et al., "Compression of 1.8 μm laser pulses to sub-two optical cycles with bulk material," *Appl. Phys. Lett.*, vol. 96, 2010, Art. no. 121109.

[63] B. E. Schmidt et al., "CEP stable 1.6 cycle laser pulses at 1.8 μm," *Opt. Exp.*, vol. 19, pp. 6858–6864, 2011.

[64] P. Béjot, B. E. Schmidt, J. Kasparian, J.-P. Wolf, and F. Legaré, "Mechanism of hollow-core-fiber infrared-supercontinuum compression with bulk material," *Phys. Rev. A*, vol. 81, 2010, Art. no. 063828.

[65] G. Fan et al., "Hollow-core-waveguide compression of multi-millijoule CEP-stable 3.2 μm pulses," *Optica*, vol. 3, pp. 1308–1311, 2016.

[66] T. Nagy, L. von Grafenstein, D. Ueberschaer, and U. Griebner, "Femtosecond multi-10-mJ pulses at 2 μm wavelength by compression in a hollow-core fiber," *Opt. Lett.*, vol. 46, pp. 3033–3036, 2021.

[67] M. Chergui, "Ultrafast molecular photophysics in the deep-ultraviolet," *J. Chem. Phys.*, vol. 150, 2019, Art. no. 070901.

[68] C. G. Durfee III, S. Backus, H. C. Kapteyn, and M. Murnane, "Intense 8-fs pulse generation in the deep ultraviolet," *Opt. Lett.*, vol. 24, pp. 697–699, 1999.

[69] L. Misoguti et al., "Generation of broadband VUV light using third-order cascaded processes," *Phys. Rev. Lett.*, vol. 87, 2001, Art. no. 013601.

[70] D. J. Kane and R. Trebino, "Characterization of arbitrary femtosecond pulses using frequency-resolved optical gating," *IEEE J. Quantum Electron.*, vol. 29, no. 2, pp. 571–579, Feb. 1993.

[71] S. Backus et al., "16-fs, 1-μJ ultraviolet pulses generated by third-harmonic conversion in air," *Opt. Lett.*, vol. 21, pp. 665–667, 1996.

[72] P. Tzankov et al., "High-power fifth-harmonic generation of femtosecond pulses in the vacuum ultraviolet using a ti:sapphire laser," *Opt. Exp.*, vol. 15, pp. 6389–6395, 2007.

[73] R. Forbes, Q. Leterrier, P. Hockett, and R. Lausten, "Efficient generation of vacuum ultraviolet femtosecond pulses via four-wave mixing," presented at the Conf. Frontiers in Optics 2023, Tacoma, WA, USA, 2023, Paper JTu4A.32.

[74] Y. Jiang et al., "Ultraviolet pulse compression via cross-phase modulation in a hollow-core fiber," *Optica*, vol. 11, pp. 291–296, 2024.

[75] T. Nagy and P. Simon, "Generation of 200-μJ, sub-25-fs deep-UV pulses using a noble-gas-filled hollow fiber," *Opt. Lett.*, vol. 34, pp. 2300–2302, 2009.

[76] J. C. Travers, T. F. Grigorova, C. Brahms, and F. Belli, "High-energy pulse self-compression and ultraviolet generation through soliton dynamics in hollow capillary fibres," *Nature Phot.*, vol. 13, pp. 547–554, 2019.

[77] F. Köttig et al., "Generation of microjoule pulses in the deep ultraviolet at megahertz repetition rates," *Optica*, vol. 4, pp. 1272–1276, 2017.

[78] P. K. A. Wai, C. R. Menyuk, Y. C. Lee, and H. H. Chen, "Nonlinear pulse propagation in the neighborhood of the zero-dispersion wavelength of monomode optical fibers," *Opt. Lett.*, vol. 4, pp. 464–466, 1986.

[79] V. I. Karpman, "Radiation by solitons due to higher-order dispersion," *Phys. Rev. E*, vol. 47, pp. 2073–2082, 1993.

[80] N. Akhmediev and M. Karlsson, "Cherenkov radiation emitted by solitons in optical fibers," *Phys. Rev. A*, vol. 51, pp. 2602–2607, 1995.

[81] J. N. Elgin, T. Brabec, and S. M. J. Kelly, "A perturbative theory of soliton propagation in the presence of third order dispersion," *Opt. Commun.*, vol. 114, pp. 321–328, 1995.

[82] M. Reduzzi et al., "Direct temporal characterization of sub-3-fs deep UV pulses generated by resonant dispersive wave emission," *Opt. Exp.*, vol. 31, 2023, Art. no. 26854.

[83] C. Brahms, F. Belli, and J. C. Travers, "Resonant dispersive wave emission in hollow capillary fibers filled with pressure gradients," *Opt. Lett.*, vol. 45, pp. 4456–4459, 2020.

[84] J. K. Wahlstrand, Y.-H. Cheng, and H. M. Milchberg, "Absolute measurement of the transient optical nonlinearity in N -2, O_2, N_2 O,and AR," *Phys. Rev. A*, vol. 85, 2012, Art. no. 043820.
[85] M. Nisoli et al., "A novel high-energy pulse compression system: Generation of multigigawatt sub-5-fs pulses," *Appl. Phys. B*, vol. 65, pp. 189–196, 1997.
[86] C. H. Lin, J. P. Heritage, T. K. Gustafson, R. Y. Chiao, and J. P. McTague, "Birefringence arising from the reorientation of the polarizability anisotropy of molecules in collisionless gases," *Phys. Rev. A*, vol. 13, pp. 813–829, 1976.
[87] J. F. Ripoche et al., "Determination of the time dependence of n_2 in air," *Opt. Commun.*, vol. 135, pp. 310–314, 1997.
[88] J. E. Beetar et al., "Multioctave supercontinuum generation and frequency conversion based on rotational nonlinearity," *Sci. Adv.*, vol. 6, 2020, Art. no. eabb5375.
[89] R. Safaei et al., "High-energy multidimensional solitary states in hollow-core fibres," *Nature Photon.*, vol. 14, pp. 733–741, 2020.
[90] M. Nisoli et al., "Single-electron subpicosecond coherent dynamics in KBr f. centers," *Phys. Rev. Lett.*, vol. 77, pp. 3463–3466, 1996.
[91] C. Spielmann et al., "Generation of coherent x-rays in the water window using 5-Femtosecond laser pulses," *Science*, vol. 278, pp. 661–664, 1997.
[92] M. Ferray et al., "Multiple-harmonic conversion of 1064 nm radiation in rare gases," *J. Phys. B*, vol. 21, pp. L31–L35, 1988.
[93] J. L. Krause, K. J. Schafer, and K. C. Kulander, "High-order harmonic generation from atoms and ions in the high intensity regime," *Phys. Rev. Lett.*, vol. 68, pp. 3535–3538, 1992.
[94] T. Brabec and F. Krausz, "Intense few-cycle laser fields: Frontiers of nonlinear optics," *Rev. Mod. Phys.*, vol. 72, pp. 545–591, 2000.
[95] F. Calegari, G. Sansone, S. Stagira, C. Vozzi, and M. Nisoli, "Advances in attosecond science," *J. Phys. B: At., Mol. Opt. Phys.*, vol. 49, Art. no. 062001, 2016.
[96] M. Hentschel et al., "Attosecond metrology," *Nature*, vol. 414, pp. 509–513, 2001.
[97] I. J. Sola et al., "Controlling attosecond electron dynamics by phase-stabilized polarization gating," *Nature Phys.*, vol. 2, pp. 319–322, 2016.
[98] G. Sansone et al., "Isolated single-cycle attosecond pulses," *Science*, vol. 314, pp. 443–446, 2006.
[99] F. Ferrari et al., "High-energy isolated attosecond pulses generated by above-saturation few-cycle fields," *Nature Phot.*, vol. 4, pp. 875–879, 2010.
[100] G. Sansone, L. Poletto, and M. Nisoli, "High-energy attosecond light sources," *Nature Phot.*, vol. 5, pp. 655–663, 2011.
[101] P. Agostini, F. Fabre, G. Mainfray, G. Petite, and N. Rahman, "Free-free transitions following six-photon ionization of xenon atoms," *Phys. Rev. Lett.*, vol. 42, pp. 1127–1130, 1979.
[102] F. Grasbon et al., "Above-threshold ionization at the few-cycle limit," *Phys. Rev. Lett.*, vol. 91, 2003, Art. no. 173003.
[103] G. G. Paulus, F. Grasbon, H. Walther, R. Kopold, and W. Becker, "Channel-closing-induced resonances in the above-threshold ionization plateau," *Phys. Rev. A*, vol. 64, 2001, Art. no. 021401(R).

Mauro Nisoli has been a Full Professor with the Politecnico di Milano, Milan, Italy, since 2011. From 1990 to 2000, he was a Researcher of the National Research Council (CNR), Center of Quantum Electronic and Electronic Instrumentation. From 2001 to 2010, he was an Associate Professor with the Department of Physics, Politecnico di Milano. He is currently the Head of the Attosecond Research Center with the Department of Physics, Politecnico, Milan, Italy, and he is also the co-Director with International School "The Frontiers of Attosecond and Ultrafast X-ray Science". He has authored about 220 research papers in international journals and several invited and tutorial communications at international meetings and schools. His research interests include attosecond science, ultrashort-pulse laser technology, and control and real-time observation of electronic motion in atoms, molecules and solids. He was the recipient of an European Research Council (ERC) Advanced Grant in 2009 (Electron-scale dynamics in chemistry, ELYCHE) and an ERC Synergy Grant in 2020 (The ultimate time scale in organic molecular opto-electronics, the attosecond, TOMATTO). He is OSA Fellow for innovative contributions to the field of attosecond science and technology, particularly for ground-breaking applications of attosecond pulses to molecules.

Open Access funding provided by 'Politecnico di Milano' within the CRUI CARE Agreement